



# HHS Public Access

Author manuscript

*Int J Min Sci Technol.* Author manuscript; available in PMC 2020 June 05.

Published in final edited form as:

*Int J Min Sci Technol.* 2020 ; 30(1): 17–24.

## Loading characteristics of mechanical rib bolts determined through testing and numerical modeling

Khaled Mohamed<sup>a,\*</sup>, Gamal Rashed<sup>a</sup>, Zorica Radakovic-Guzina<sup>b</sup>

<sup>a</sup>Centers for Disease Control, National Institute for Occupational Safety and Health, Pittsburgh, PA 15236, USA

<sup>b</sup>ITASCA Consulting Group, Minneapolis, MN 55401, USA

### Abstract

Underground coal mines use mechanical bolts in addition to other types of bolts to control the rib deformation and to stabilize the yielded coal ribs. Limited research has been conducted to understand the performance of the mechanical bolts in coal ribs. Researchers from the National Institute for Occupational Safety and Health (NIOSH) conducted this work to understand the loading characteristics of mechanical bolts (stiffness and capacity) installed in coal ribs at five underground coal mines. Standard pull-out tests were performed in this study to define the loading characteristics of mechanical rib bolts. Different installation torques were applied to the tested bolts based on the strength of the coal seam. A typical tri-linear load-deformation response for mechanical bolts was obtained from these tests. It was found that the anchorage capacity depended mainly on the coal strength. Guidelines for modeling mechanical bolts have been developed using the tri-linear load-deformation response. The outcome of this research provides essential data for rib support design.

### Keywords

Coal rib; Mechanical bolt; Conventional bolt; Tension bolt; Point-anchored bolt; Rib support; Pull-out test; Numerical modeling; FLAC3D

## 1. Introduction

The design of rib bolting in United State coal mines is based on a trial and error process, which is insufficient to eliminate injuries and fatalities caused by rib falls. In the last decade, rib failures have resulted in 17 fatalities, representing 52% of the ground-fall fatalities in underground coal mines in the United States [1]. Recently, researchers from the National Institute for Occupational Safety and Health (NIOSH) surveyed 90 sites in 14 underground coal mines in the Eastern United States and found that 11 mines are bolting coal ribs, of which 4 mines use the conventional mechanical bolts and the others use fully-grouted bolts. NIOSH researchers are developing an engineering design procedure for rib support. Pull-out

This is an open access article under the CC BY-NC-ND license (<http://creativecommons.org/licenses/by-nc-nd/4.0/>).

\*Corresponding author. kmy1@cdc.gov (K. Mohamed).

test program for mechanical and grouted rib bolts were conducted to understand the rib control mechanisms of rib bolts. Only the test results of mechanical bolts are presented in this paper.

The mechanical bolt (or point-anchored bolt) is a tensioned bolt anchored down the borehole with a mechanical expansion shell or a resin-grouted medium [2]. The mechanical anchor bolt consists of a plug, a shell anchor, a headed bar with the top end threaded, a bearing plate, a hardened washer, and sometimes a friction-reducing washer. The shell anchor can be either standard or bail type, as shown in Fig. 1. The standard type shell is held in place by a nut, while the bail anchor uses a strap to hold the shell in place [3]. The diameter of the bar is generally 16 mm for the #5 bolt or 19 mm for the #6 bolt. The diameter of the hole that the bolt is inserted into must be carefully controlled since an oversized hole can result in poor anchorage [4]. The anchorage is obtained by applying torque to the bolt head, which in turn pulls the plug down in the shell and expands the serrated leaves against the sides of the hole-wall. In the resin-grouted anchor, the resin replaces the mechanical expansion shell at the end of the hole. The anchorage is achieved by bonding between the resin, bolt, and the hole-wall.

The anchorage capacity and the shear stiffness are the key parameters that govern the behavior of mechanically anchored bolts. Standard pull-out tests can be used to determine the anchorage capacity and the shear stiffness of the anchorage. The anchorage capacity is defined as the load at which an excessive anchorage slippage or yielding of the bolt occurs. Howe analyzed the factors affecting the anchorage performance of the expansion shell and found that the anchorage capacity increased with increasing plug angle and bearing area of the leaves [5].

Tadolini conducted 37 pull-out tests on bolts in a coal roof [6]. Roof bolts are used to create a thick, strong beam by strengthening thin roof layers or by suspending the immediate roof in a strong roof stratum. On the other hand, rib bolts are applied to contain yielded ribs in place and to control rib deformation. Hence, these conclusions from Tadolini do not necessarily apply to ribs [6]. Hebblewhite studied the applications of rib bolts in Australian mines and concluded that the standard roof support practices were not directly applicable to ribs control [7]. Limited research has been conducted to understand how a mechanical anchor performs in a coal rib. Larson and Dunford conducted 220 pull-out tests for expansion-shell mechanical rib bolts in two coal seams in two different mines and found that the anchorage system showed a bilinear response during the pull-out test, and the condition of the rib, e.g., age and coal strength, was the most significant factor in determining the mechanical anchorage capacity [8]. However, Larson and Dunford did not provide an explanation for the bilinear model they found from the test results [8].

Numerical modeling techniques are used extensively to investigate the mechanisms of interaction between rock bolts and rock mass. Numerous finite element and finite difference models have previously been developed to numerically model the fully grouted bolts in mine applications [9–13]. On the other hand, a few efforts were committed to numerically model mechanical bolts in mine applications. For example, Zhang and Peng explicitly modeled mechanical bolts as beam elements in which the anchor was modeled by tying the end nodes

of the bolt to the surrounding rock and the bearing plate was in contact with the rock surface [14]. The pre-tension is simulated by an assembly load so that the mechanical bolt will act like a fastener in responding to active pre-tension.

The behavior of mechanical expansion anchor bolts in coal pillar ribs was studied in this paper and a detailed explanation of the main parameters required to obtain a successful rib support design was provided. The study explored the factors affecting the anchorage capacity and the stiffness of the mechanical bolts and introduced a torque-tension model based on the best fit for experimental pull-out test results. Guidelines for modeling mechanical bolts have been developed using the tri-linear bolt load-deformation response. The outcome of this research improves understanding of how a mechanical anchor performs in a coal rib and provides essential data for rib support design.

## 2. Torque-tension relationship of mechanical bolts

During the installation of mechanical bolts, an installation torque is applied on the head of the bolt. The applied torque is transformed into uniform tension in the bar between the shell at the end of the bolt and the bearing plate set against the rib. The relationship between the applied torque and the induced tension is called the torque-tension ratio. This ratio is highly affected by the mechanical details of the bolt/anchor/bearing plate assembly [3]. To maximize the torque-tension ratio, a friction-reducing washer is placed between the bearing plate and the bolt head. The applied tension is activated immediately to build the compression zone in the supported rib along the bar length. Six bail-type mechanical bolts of 16 mm diameter and 1.2 m long were installed in the coal seam of the NIOSH Safety Research Coal Mine, Pittsburgh, PA. The torque-tension relationship provided by the manufacturer of the tested mechanical bolt (dashed line in Fig. 2) is given by the following linear model equation:

$$P = 0.27 * T \quad (1)$$

where  $P$  is the bolt tension; and  $T$  the bolt installation torque.

The torque-tension ratio of the tested mechanical bolts was determined experimentally in this study. The installation torque was applied manually using a calibrated torque wrench as shown in Fig. 3. A load cell was used to measure the induced tension in the bolt. The relationship between the applied torque and the induced tension in the tested bolts is non-linear as shown in Fig. 2. The scatter of test points is explained by the heterogeneity of the coal. The best fit for the torque-tension relationship is given by the following non-linear model equation:

$$P = 0.778 * T^{0.671} \quad (2)$$

The induced tensions in the tested bolts at a torque greater than 102 kN-mm were consistently smaller than those calculated by the manufacturer's formula (Eq. (1)). The reduction in the torque-tension ratio could be explained by the following: (1) loss of tension due to friction between the pull collar and other parts, and/or (2) coal yielding at the anchor-

end because of induced high radial stresses and relatively low coal strength of 15.53 MPa. In the future, the torque-tension relationship will be obtained for stronger coal.

### 3. Pull-out tests of mechanical bolts

The standard roof bolt anchorage testing procedure was followed to conduct the pull-out tests for mechanical bolts installed in coal ribs [15]. A standard pull gear was used to determine the load-displacement curves of the tested bolts. Fig. 4 shows a schematic drawing of the components of the standard pull gear. Pull-out tests were conducted for the bail-type mechanical bolts of 19 mm diameter and 1.2 m long installed in the NIOSH Safety Research Mine's coal seam in Pittsburgh, PA. The NIOSH research mine is an old room-and-pillar mine in the Pittsburgh coal seam. Bolts were manually torqued to 68 kN-mm using a calibrated torque wrench. Fig. 5 shows the pull gear mounted on the pre-tensioned rib bolt before testing and the loading cell sandwiched between two loading plates. The load applied on the bolt is recorded simultaneously by the load cell (Fig. 4) and the pressure transducer connected to the hydraulic jack (Fig. 4).

Fig. 6 shows a typical load-displacement curve for a tested rib bolt (the bolt load recorded by the load cell is marked by dashed lines, and the jack load recorded by the pressure transducer is marked by a solid line). The cell load-displacement curve shows the actual bolt loading and bolt/coal interaction during the pull-out test. Generally, the standard pull gear does not include the load cell. Hence, the jack load-displacement curve is a typical load-displacement behavior for standard pull-out tests. Three distinct portions (Line *a-b*, Line *b-c* and Line *c-e*, respectively, in Fig. 6) may be identified in the jack load-displacement curve:

1. The first portion (Line *a-b*) is between the initial application of jack load (Point *a*) and the point at which the jack load and the cell load become equal (Point *b*). At Point *a*, the jack load begins to transfer to the bolt. Up until Point *a*, slack is being taken out of the test equipment. Line *a-b* has no significance for the anchorage mechanism of the mechanical bolt other than to indicate the point at which the jack load and the cell load became equal (Point *b*).
2. The center portion (Line *b-c*) begins where the jack load and the cell load coincide and then increases linearly. The slope of Line *b-c* is a measure of the shear stiffness of the shell/coal anchorage. The shear stiffness of the mechanical anchorage is calculated as 1051 kN/m. The standard roof bolt anchorage testing procedure defines the intercept (Point *d*) of the center portion (Line *b-c*) as a good approximation for the pre-tension load. The approximated pre-tension load was found to be 15.82 kN, while the actual pre-tension load (Point *d*) measured by the load cell was 12.18 kN. The suggested approximation of the pre-tension load overestimates the actual pre-tension load by about 30%.
3. In the flat portion (Line *c-e*) where the anchorage capacity is reached, the anchor slips when additional load is applied. The measured anchorage capacity of the tested bolt ranges from 35.11 to 36.00 kN. At Point *c*, the calculated shear stresses induced at the borehole wall became greater than or equal to the in-situ

shear strength of coal. The ultimate shear stress at the shell/coal interface is approximated by the following equation:

$$\tau = \frac{T}{f \times \pi \times D \times L} \quad (3)$$

where  $\tau$  is the ultimate shear stress;  $T$  the anchorage capacity;  $D = 35$  mm the diameter of the shell/hole;  $L = 51$  mm the length of the shell; and  $f = 0.56$  the shell/coal contact factor which represents the effective surface area of shell leaf.

Accordingly, the ultimate shear stress of the tested bolt ranges from 11.26 to 11.54 MPa. The associated radial stress at the shell/coal interface is approximated by the following equation [16]:

$$\sigma_r = \frac{\tau}{\tan(a + \varphi_b)} \quad (4)$$

where  $\sigma_r$  is the associated radial stress;  $a = 14^\circ$  the taper angle of the cone/leaf interface; and  $\varphi_b = 8.5^\circ$  the friction angle at the cone/leaf interface.

Based on Eq. (4), the ultimate radial stress of the tested bolt ranges from 27.19 to 27.88 MPa. Mohamed determined the in-situ strength of the coal at the test site using the borehole shear test [17]. The in-situ cohesion and friction angle of the coal at the test site are found to be 1.91 MPa and  $18.5^\circ$ , respectively. The in-situ shear strength of the coal material at radial stresses of 27.19 and 27.88 MPa are 11.01 and 11.23 MPa, respectively. The calculated in-situ shear strength is approximately equal to the ultimate shear stress calculated by Eq. (3).

#### 4. Typical load-displacement model for mechanical bolts

Following the initial tests described above, a study was conducted to develop a typical load-displacement model for mechanical bolts installed in coal ribs. The study was conducted at five underground coal mines of a wide range of intact strength values: the Pittsburgh, Kellioka, and Pocahontas No. 3 coal seams. Three study mines are operating in the Pittsburgh coal seam, and one study mine is operating in each of the other seams. In this study, pull-out tests were conducted for bail-type mechanical bolts with a 51 mm shell. The diameter of the tested bolts was 16 mm installed in 35 mm holes. The yield strength of tested bolts is 517 MPa. The length of the tested bolts was 1.2 m, except those installed in the Pocahontas No. 3 seam which was 1.5 m long. The range of installation torques tested depended on the accessibility and time allowed at the study sites. The critical points of the tri-linear models of all pull-out tests are listed in Table 1. Nine bolts were tested at the NIOSH Safety Research Mine. The strength of 76 mm coal cubes taken from the test site is 17.24 MPa. Three levels of installation torque were tested: 102, 136, and 163 kN-mm. The pull-out tests were repeated three times at each level of installation torque (see Table 1). Fig. 7a shows samples of the measured load-displacement curves for each installation torque and the approximated tri-linear load-displacement models (marked in dashed lines). The critical points of the tri-linear models are marked by letters *a-e* in Fig. 7a.

Mine A operates in the Pocahontas No. 3 seam at a depth greater than 610 m. The intact strength of coal samples taken from the test site is 5.79 MPa. The coal strength at Mine A is the lowest in the study. Only full-grouted bolts are used by mine operators to support coal ribs at the study site. Because of the relatively low intact strength of the coal in the Pocahontas No. 3 seam and the large depth of the study site, it was decided to test 1.5 m long mechanical bolts to place the anchor in solid coal. Despite having longer bolts installed at Mine A, it was difficult to maintain the installation torque. Therefore, only two bolts were installed at a torque of 102 kN-mm. The critical points of the tri-linear load-displacement models (marked in dashed lines) are shown in Fig. 7b.

Like the NIOSH Safety Research Mine, Mine B and Mine C are operating in the Pittsburgh coal seam. Only one level of installation torque was tested in these mines because of limited accessibility. A total of three pull-out tests were conducted at both Mine B and Mine C. The installation torque for all tests was 136 kN-mm, except for one test at 163 kN-mm. Fig. 7c and d show the measured load-displacement curves and the approximated tri-linear load-displacement models (marked in dashed lines) at Mine B and Mine C, respectively.

Mine D is operating in the Kellioka coal seam, which is the strongest seam in this study. The intact strength at the study site is 31.95 MPa. It was decided to install three bolts at a high torque of 163 kN-mm because of high coal strength. At Mine D, it was not difficult to identify the critical points of the tri-linear load-displacement models (marked in dashed lines) as shown in Fig. 7e. The anchorage capacity of 80–98 kN at Mine D is the highest in this study.

Statistical software was used to examine the effects of the coal strength and the installation torque on the measured capacity and shear stiffness of the anchorage [19]. A null hypothesis of no correlation between the studied variables was tested. A scatterplots matrix representing the correlations between the studied variables is shown in Fig. 8. It is apparent that there is a strong positive correlation between the anchorage capacity and the intact strength of coal where the correlation coefficient ( $r$ ) is 0.92. Also, there is a weak positive correlation between the anchorage capacity and the installation torque ( $r=0.57$ ) and a relatively weak positive correlation between the shear stiffness of the anchorage and the installation torque ( $r=0.72$ ). The p-values for all correlation coefficients were less than 0.01 which means that all of them are statistically significant.

In summary, typical load-displacement curves have been deduced from the pull-out test study conducted for bail-type mechanical bolts. Fig. 9 shows the typical tri-linear load-displacement models of the mechanical bolts for two levels of installation torques ( $T_1 < T_2$ ). The key features of the typical tri-linear load-displacement models are:

1. Up until Point *a*, slack is being taken out of the test equipment.
2. Line *a-b* has no significance for the anchorage mechanism of the mechanical bolt other than to indicate the point at which the jack load and the cell load become equal (Point *b*).
3. The pre-tension load (*P*) is non-linear correlated with the installation torque (*T*) as presented in Eq. (2). The pre-tension load (Point *d*) can be approximated as

70% of the intercept of the second segment of the tri-linear load-displacement model (Point  $d'$ ).

4. The coal/mechanical bolt interaction can be simplified as a combination of three springs connected in series; the first spring represents the stiffness of the bar, the second spring represents the interaction between the cone and shell leaves, and the third spring represents the interaction between the shell leave and coal. For simplicity, it was assumed that the bearing plate would be in contact with coal without serration during the test and very limited coal yielding would be observed at the bearing plate. Therefore, the effect of the coal/bearing plate interaction can be ignored. The coal at the anchorage point is intact during the first segment of the tri-linear load-displacement model (Line  $d-b$ ), and the leaves of the shell are in full contact with the hosting coal. The bolt head displacement in the first segment is the summation of the bolt elongation and displacement of the cone. Therefore, the slope of the first segment ( $K_{db}$ ) is governed by the stiffness of the bar ( $K_b$ ) and the stiffness of cone/leaf interface ( $K_s$ ) as follows:

$$K_{db} = \frac{K_b \times K_s}{K_b + K_s} \quad (5)$$

$$K_b = \frac{E_b \times A_b}{L_b} \quad (6)$$

where  $E_b$  is the Young's modulus of steel;  $A_b$  the cross-sectional area of the bolt; and  $L_b$  the length of the bolt.

5. At the anchorage point, the coal gradually yields in the second segment of the tri-linear load-displacement model (Line  $b-c$ ). The slope of the second segment ( $K_{bc}$ ) depends on the stiffness of the bolt ( $K_b$ ), the stiffness of the cone/leaf interface ( $K_s$ ), and the stiffness of the yielded coal ( $K_c$ ) as follows:

$$K_{bc} = \frac{K_b \times K_s \times K_c}{K_b \times K_c + K_s \times K_b + K_s \times K_c} \quad (7)$$

6. The slope of the second segment of the tri-linear load-displacement model ( $K_{bc}$ ) is independent of the installation torque.
7. The anchorage capacity (Point  $c$ ) is independent of the installation torque. The anchorage capacity depends on the strength of the hosting coal and the geometry of the shell (length and diameter) as formulated in Eqs. (1) and (2).

## 5. Guidelines for numerical modeling of mechanical bolts

The FLAC3D numerical code has been used in this study to develop the guidelines for modeling mechanical bolts [20]. The pull-out Test #1 at Mine B (Table 1) was used as an example for demonstrating the numerical modeling of mechanical bolts. Fig. 10 shows the recorded (raw) load-displacement curve and the corresponding tri-linear model of Test #1 at

Mine B. Fig. 11 shows the FLAC3D model for a 1.2 m long mechanical bolt installed in a 2 m cube of coal. The bearing plate installed between the bolt head and coal face is 20 mm × 20 mm and 9 mm thick.

Cable structural elements were used to model the mechanical bolt, and liner structural elements were used to model the bearing plate. The shell anchor was modeled by grouting 76 mm of the bolt-end into the coal block (anchor zone, Fig. 11). The coal block was modeled using the coal-mass modeling approach developed by Mohamed et al. [21]. Enough zones were generated in the coal block around the anchor and underneath the bearing plate to capture stress gradients in these highly stressed areas. Each coal element in the anchor zone has at least one cable element. The mechanical properties of the mechanical bolt and coal-mass are summarized in Tables 2 and 3.

The shear stiffness of the anchor varies throughout the test as shown in Fig. 10. In the first segment of the test (Line *d-b*), the stiffness of the anchor (anchor stiffness<sub>1</sub>) is approximated by the stiffness of the cone/leaf interface ( $K_s$ ) and anchor length ( $L_{anch}$ ) by substituting in Eq. (5) as follows:

$$\text{anchor stiffness}_1 = \frac{K_s}{L_{anch}} = \frac{K_{db} \times K_b}{K_b - K_{db}} \times \frac{1}{L_{anch}} \quad (8)$$

where  $K_{db}$  is the stiffness of the first segment obtained from Fig. 10 as 9.5 MN/m;  $K_b = 34.6$  MN/m;  $L_{anch} = 0.076$  m; and anchor stiffness<sub>1</sub> = 171.3 MN/m<sup>2</sup>.

In the second segment of the pull-out test (Line *b-c*), the anchorage stiffness (anchor stiffness<sub>2</sub>) is approximated by the stiffness of yielded coal ( $K_c$ ) and anchor length ( $L_{anch}$ ) by substituting in Eq. (7) as follows:

$$\text{anchor stiffness}_2 = \frac{K_c}{L_{anch}} = \frac{K_b \times K_s \times K_{bc}}{K_s \times K_b - K_{bc} \times (K_s + K_b)} \times \frac{1}{L_{anch}} \quad (9)$$

where  $K_{bc}$  is the stiffness of the second segment obtained from Fig. 10 as 1.8 MN/m; and anchor stiffness<sub>2</sub> = 30.1 MN/m<sup>2</sup>.

A very high coupling stiffness and yield strength of 104 MN/m<sup>3</sup> and 104 MN/m<sup>2</sup>, respectively, were assigned for the liner elements to prevent the bearing plate from penetrating into coal block or separating from the coal block. The bearing plate could slide on the surface of the coal block by assigning zero cohesion and zero friction angle for the liner elements.

The model was solved in three steps. In the first step, a fixed boundary condition was assigned to the right surface of the coal block. The bolt head was rigidly tied to the bearing plate by joining the node at the bolt head to the center node of the bearing plate. A pre-tension load of 24.9 kN was applied to the free length of the bolt, then the model was solved to equilibrium. In the second step, the bond between the bolt head and bearing plate was broken, and the bolt head and bearing plate were constrained in the x-direction. The model was solved to equilibrium. In the third step, the bolt head was displaced uniformly in the



negative x-direction with a pseudo-static velocity of  $1 \times 10^{-6}$  m/s. The induced bolt load and displacement at the bolt head were recorded.

The load-displacement curve obtained by the FLAC3D model was compared with the reduced tri-linear load-displacement model of Test #2 at Mine B as shown in Fig. 10. It shows that the deduced properties (Table 2) of the mechanical bolt were sufficiently accurate to reproduce the measured load-displacement curve. Fig. 10 shows that the bolt model was pulled linearly in the first segment (Line *d-b*), and then shows non-linear behavior in the second segment (Line *d-c*). The non-linearity became more obvious when the bolt achieved its anchorage capacity (Point *c*).

## 6. Conclusions

NIOSH researchers conducted the research described in this paper to define the loading characteristics of mechanical bolts installed in coal ribs at five underground coal mines. Twenty-one grade-75 mechanical bolts of 16 mm diameter from a single manufacturer were tested in the study. The outcome of this research provides essential data for rib support design. The main findings of this study are:

1. The pull-out test mechanism for mechanical bolts was explained by measuring the induced load in the bolt via a load cell and a pressure transducer. A typical tri-linear load-deformation model was developed from pull-out tests conducted in the study mines.
2. The anchorage capacity of the mechanical bolt is directly proportional to the strength of coal.
3. The anchorage capacity of the mechanical bolt is independent of the installation torque. More pull-out tests of mechanical bolts for different installation torques are required to confirm this conclusion.
4. A non-linear torque-tension relationship was obtained from the 16-mm-diameter bail-type mechanical bolts tested coal pillars. The pre-tension load is directly proportional to the installation torque and can be approximately determined from the tri-linear load-deformation model.
5. Guidelines for modeling mechanical bolts have been developed using the tri-linear load-deformation model.

## Acknowledgements

The authors would like to thank Mr. Todd Minoski for preparing the data collection system, Mr. Craig Compton for preparing the pull-out test gear, Mr. Timothy Matthews for preparing the borehole shear test, and Mr. Daniel McElhinney, Mr. James Addis, and Ms. Cynthia Hollerich for conducting the pull-out tests.

## References

- [1]. MSHA. Preliminary accident reports, fatality alerts and fatal investigation reports. U.S. Department of Labor. Mine Safety and Health Administration; 2018.
- [2]. Peng SS, Tang DHY. Roof bolting in underground mining: a state-of-the-art review. *Int J Min Eng* 1984;2(1):1–42.

- [3]. Peng SS. Coal mine ground control. 3rd ed. Morgantown, WV: West Virginia University; 2008 p. 750.
- [4]. Moss KJ. Rock bolts in current use in Australia In: Proceeding of the symposium on rock bolting. Carlton South: the Australasian Institute of Mining and Metallurgy; 1971.
- [5]. Howe BJ. Roofbolts anchorage in mudstone. Australian Coal Industry Research Laboratories Ltd; 1968.
- [6]. Tadolini SC. Anchorage capacities in thick coal roofs. Bureau of Mines: Information Circular-United States; 1985.
- [7]. Hebblewhite BK. Years of ground control developments, practices, and issues in Australia. In: Proceedings of the 25th international conference on ground control in mining Morgantown, WV: West Virginia University; 2006 p. 111–7.
- [8]. Larson MK, Dunford JP. Two case studies of the performance of rib supports. In: Proceedings of the 15th international conference on ground control in mining Golden, CO: Colorado School of Mines; 1996 p. 527–42.
- [9]. Yassien AM, Zhang Y, Han J, Peng SS. Comparison of some aspects of bolting mechanisms between fully-grouted resin and tensioned bolts in underground mine entries. In: Proceedings of the 21st international conference on ground control in mining Morgantown, WV: West Virginia University; 2002 p. 114–25.
- [10]. Zipf RK. Numerical modeling procedures for practical coal mine design. In: Proceedings of the 41st U.S. symposium on rock mechanics (USRMS) Alexandria, VA: American Rock Mechanics Association; 2006 p. 1–11.
- [11]. Cao C, Nemcik J, Aziz N. Advanced numerical modelling methods of rock bolt performance in underground mines. In: Proceedings of the 10th underground coal operators' conference University of Wollongong & the Australasian Institute of Mining and Metallurgy; 2010 p. 326–9.
- [12]. Tulu IB, Esterhuizen GS, Heasley KA. Calibration of FLAC3D to simulate the shear resistance of fully grouted rock bolts. In: Proceedings of 46th US rock mechanics/geomechanics symposium Chicago: American Rock Mechanics Association; 2012 p. 78–88.
- [13]. Lorig LJ, Varona P. Guidelines for numerical modelling of rock support for mines. In: Proceedings of the 7th international symposium on ground support in mining and underground construction Perth: Australian Centre for Geomechanics; 2013 p. 81–105.
- [14]. Zhang Y, Peng SS. Design considerations for tensioned bolts. In: Proceedings of the 21st international conference on ground control in mining Morgantown, WV: West Virginia University; 2002 p. 131–40.
- [15]. AMC Coal Division Committee on Roof Action. Standard roof bolt anchorage testing procedure. Min Congr J 1959;45(12):59–60.
- [16]. Thompson AG, Villaescusa E. Case studies of rock reinforcement components and systems testing. Rock Mech Rock Eng 2014;47(5):1589–602.
- [17]. Mohamed K, Rashed G. Loading characteristics of mechanical rib bolts. In: Proceedings of 2019 SME annual conference and expo and CMA 121st national western mining conference Denver, CO: Society for Mining, Metallurgy and Exploration; 2019.
- [18]. Zhang Y Personal communication; 2018.
- [19]. JMP. SAS Institute Inc; 2016.
- [20]. Itasca Consulting Group. FLAC3D instruction manual. Minnesota; 2017.
- [21]. Mohamed KM, Rashed G, Sears MM, Rusnak JA, Van Dyke MA. Calibration of coal-mass model using in-situ coal pillar strength study. In: Proceedings of the vision, innovation and identity: step change for a sustainable future-2018 SME annual conference and expo and 91st annual meeting of the SME-MN section Minneapolis, MN: Society for Mining, Metallurgy and Exploration; 2018.

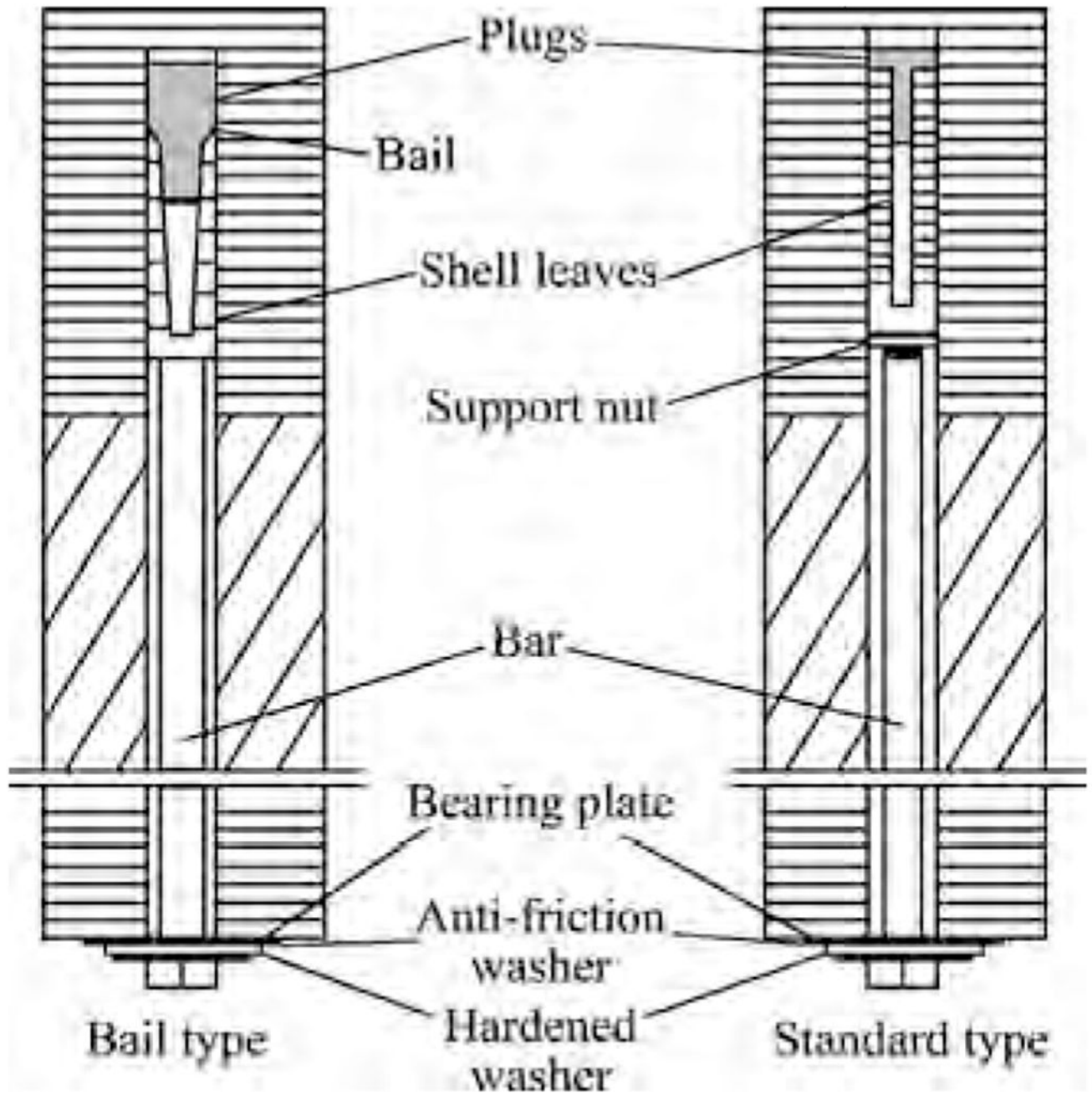


**Fig. 1.**  
Diagrams of mechanical bolts [3].

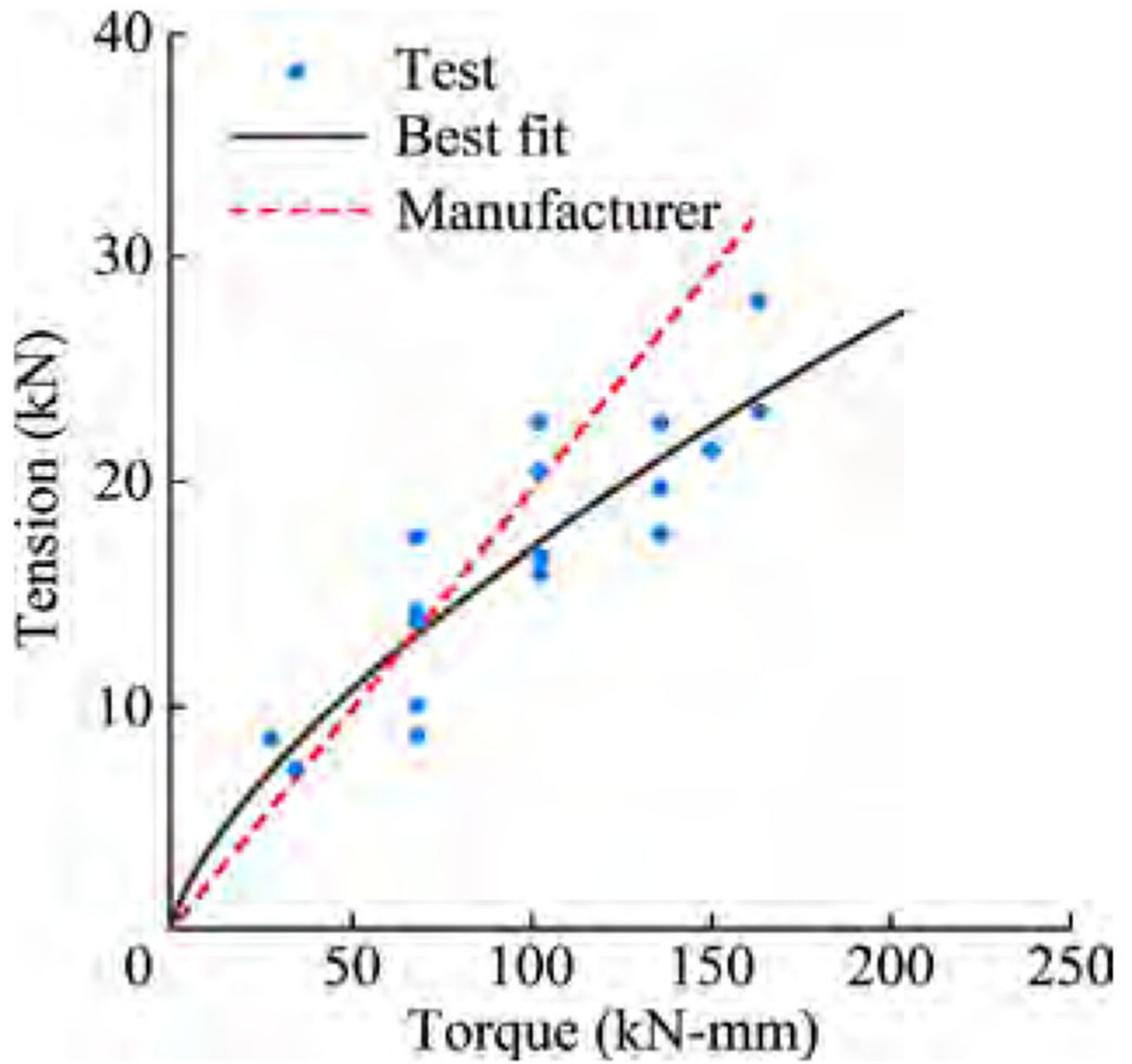


**Fig. 2.**  
Torque-tension relationship of the tested bolt.



**Fig. 3.**  
An installation torque is applied manually to the bolt.

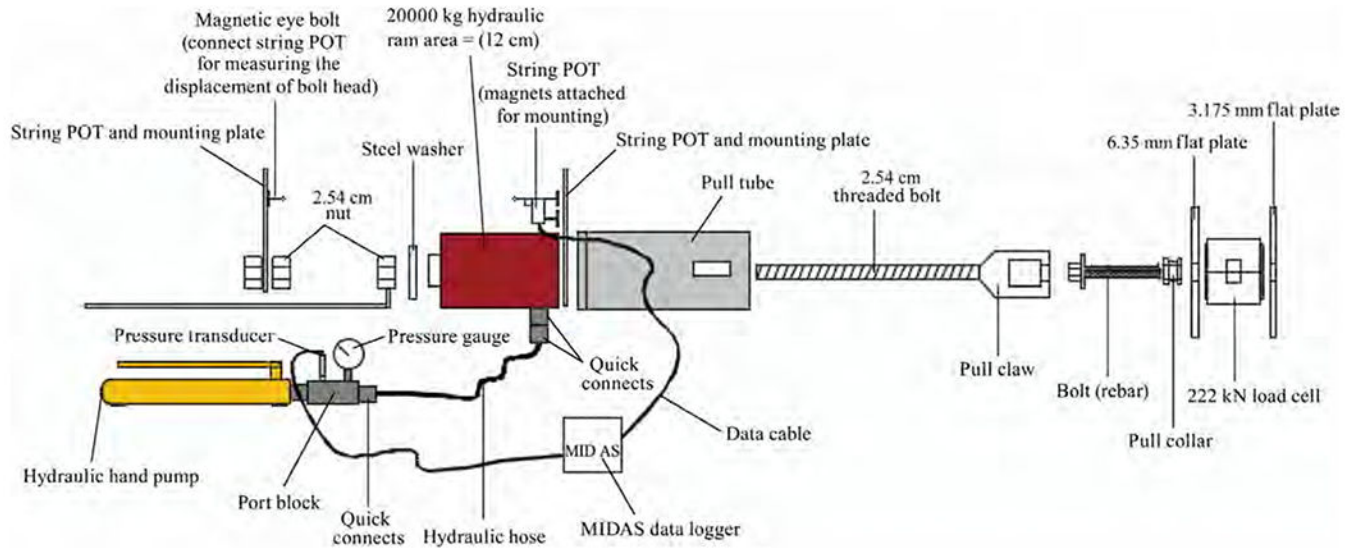


**Fig. 4.**  
Pull-out test gear components.

Author Manuscript

Author Manuscript

Author Manuscript

Author Manuscript



**Fig. 5.**  
Pull-out test gear mounted on the tested bolt.

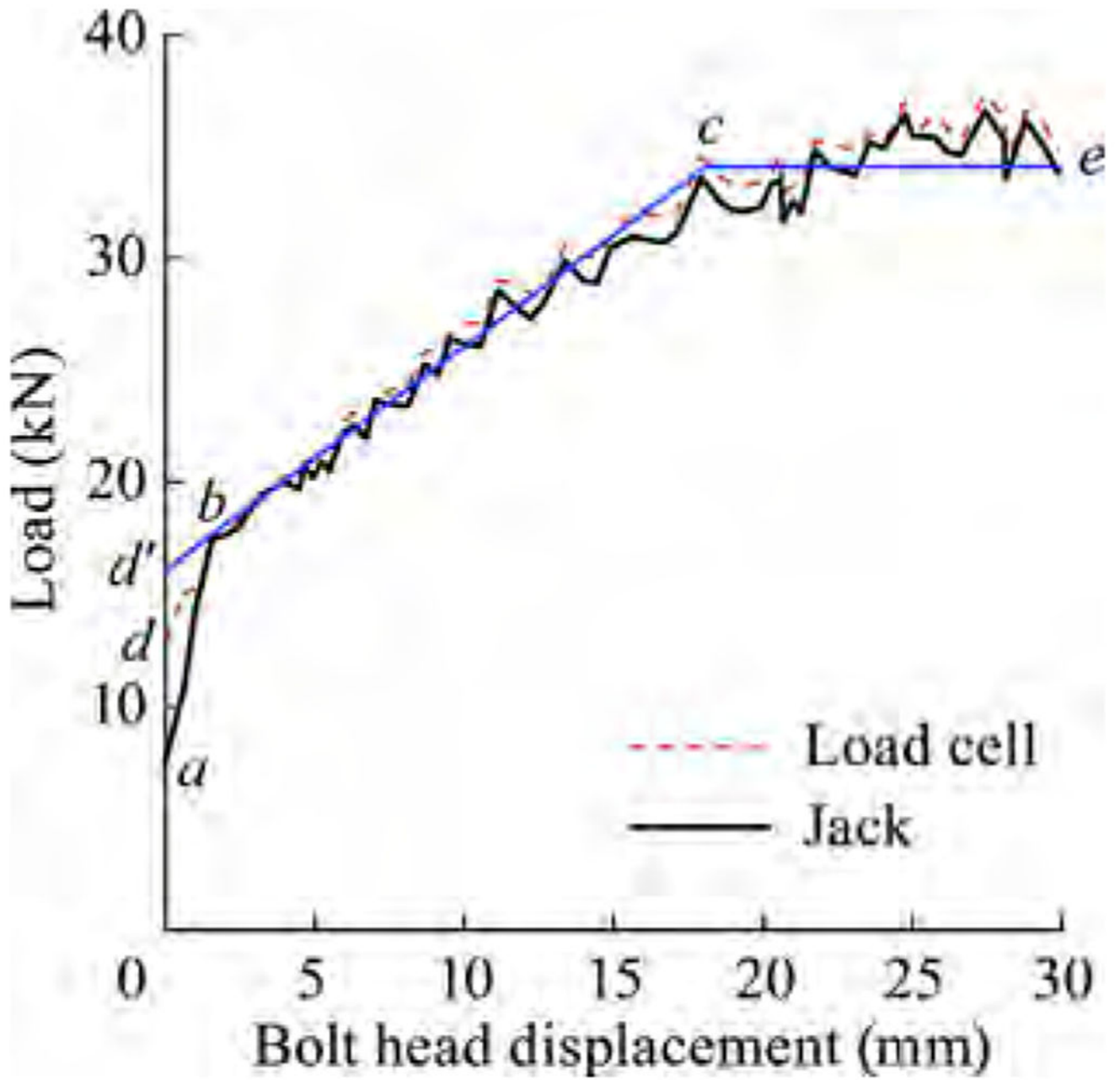
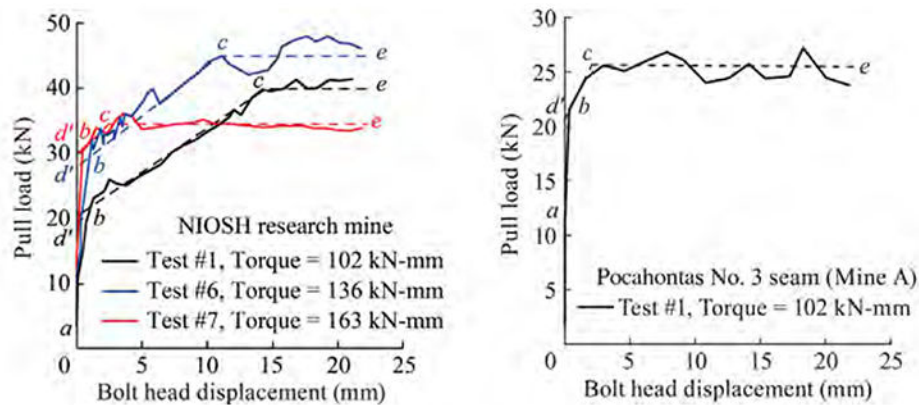


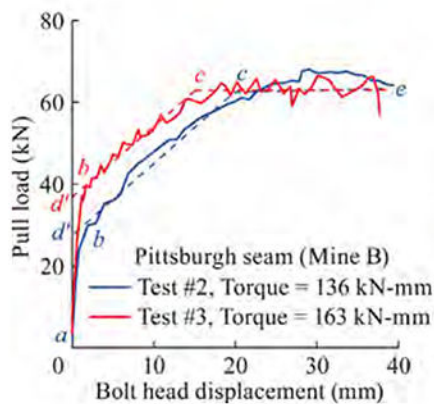
Fig. 6.  
Pull-out load-displacement curves.



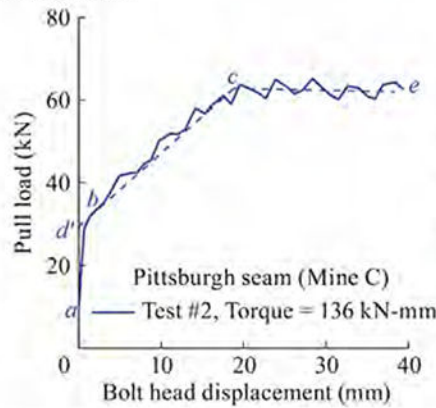


(a) NIOSH Research Mine

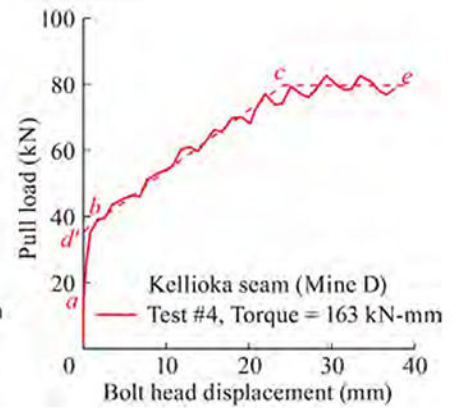
(b) Mine A



(c) Mine B



(d) Mine C



(e) Mine D

**Fig. 7.**  
Pull-out tests conducted at different coal seams.

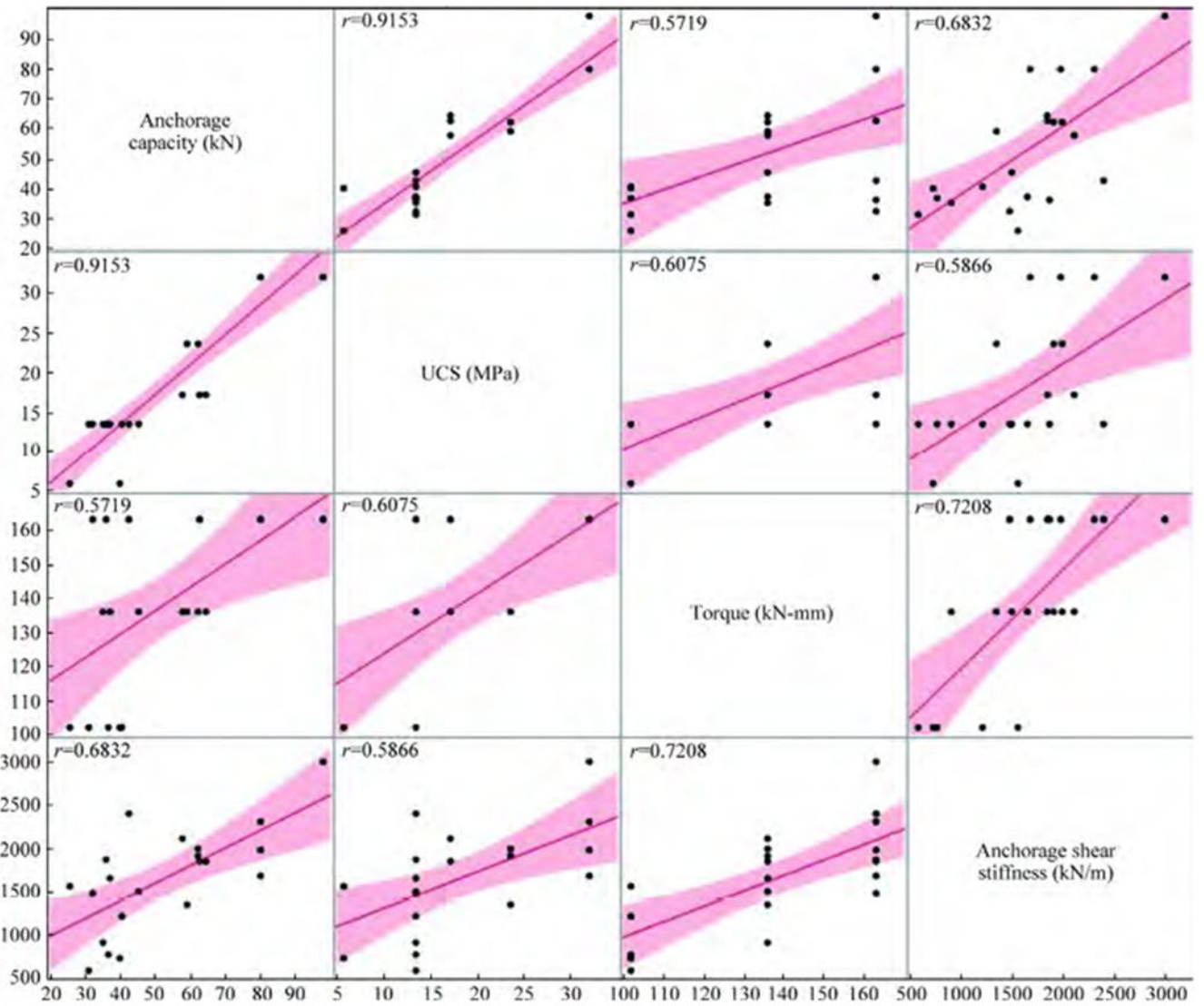


**Fig. 8.** A scatterplots matrix representing the correlations between coal strength, installation torque, capacity, and shear stiffness of the anchorage.

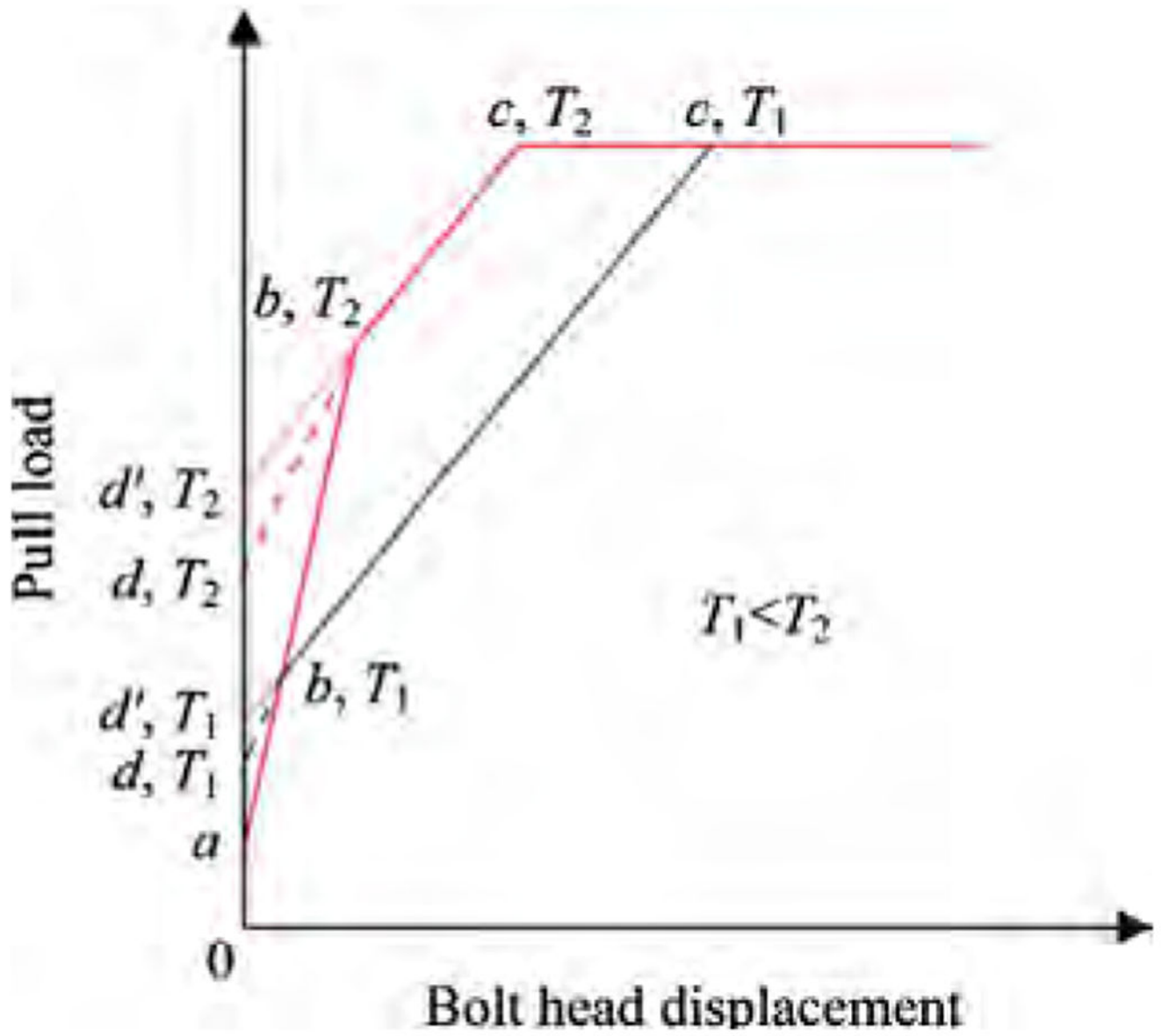
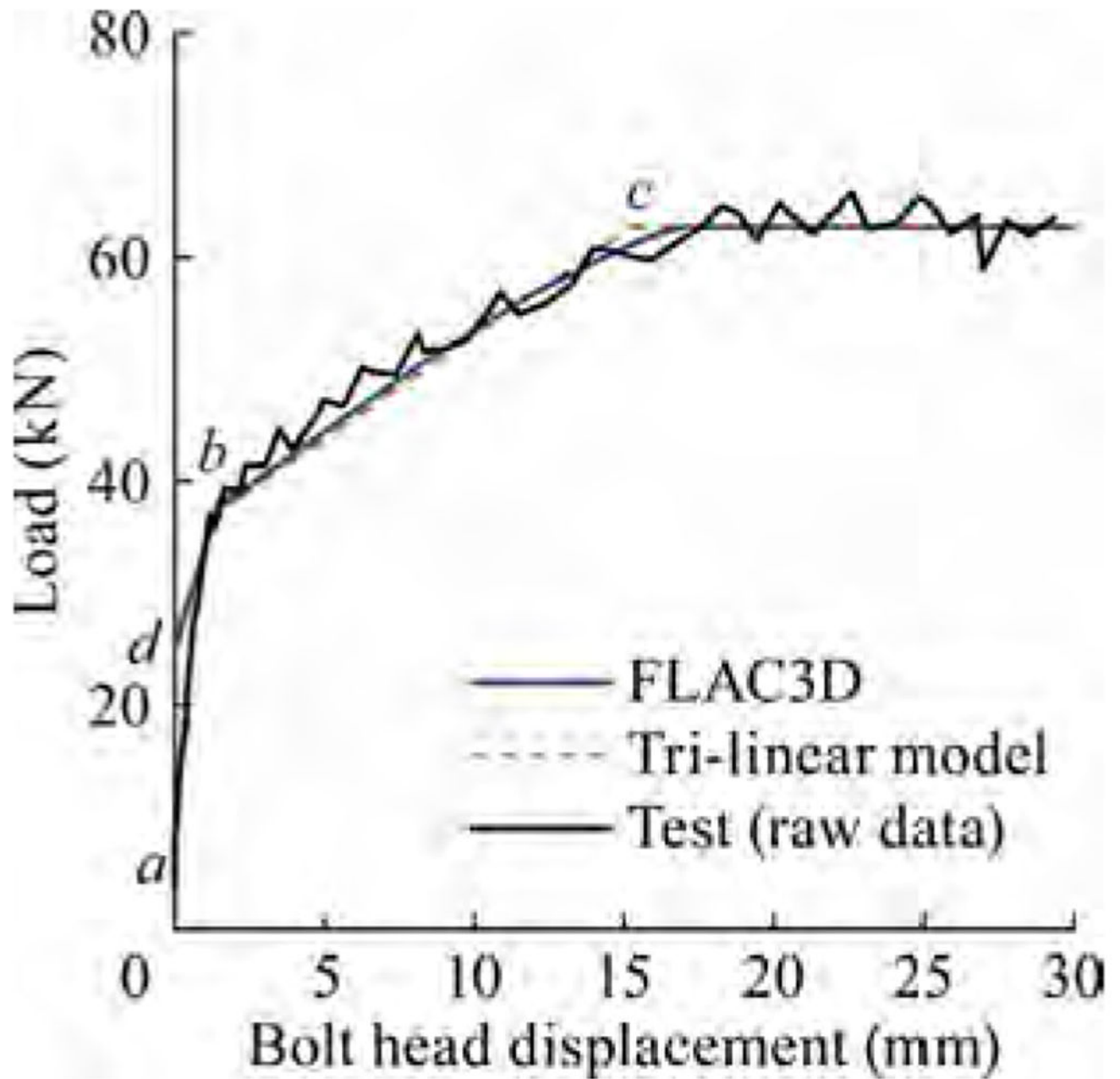
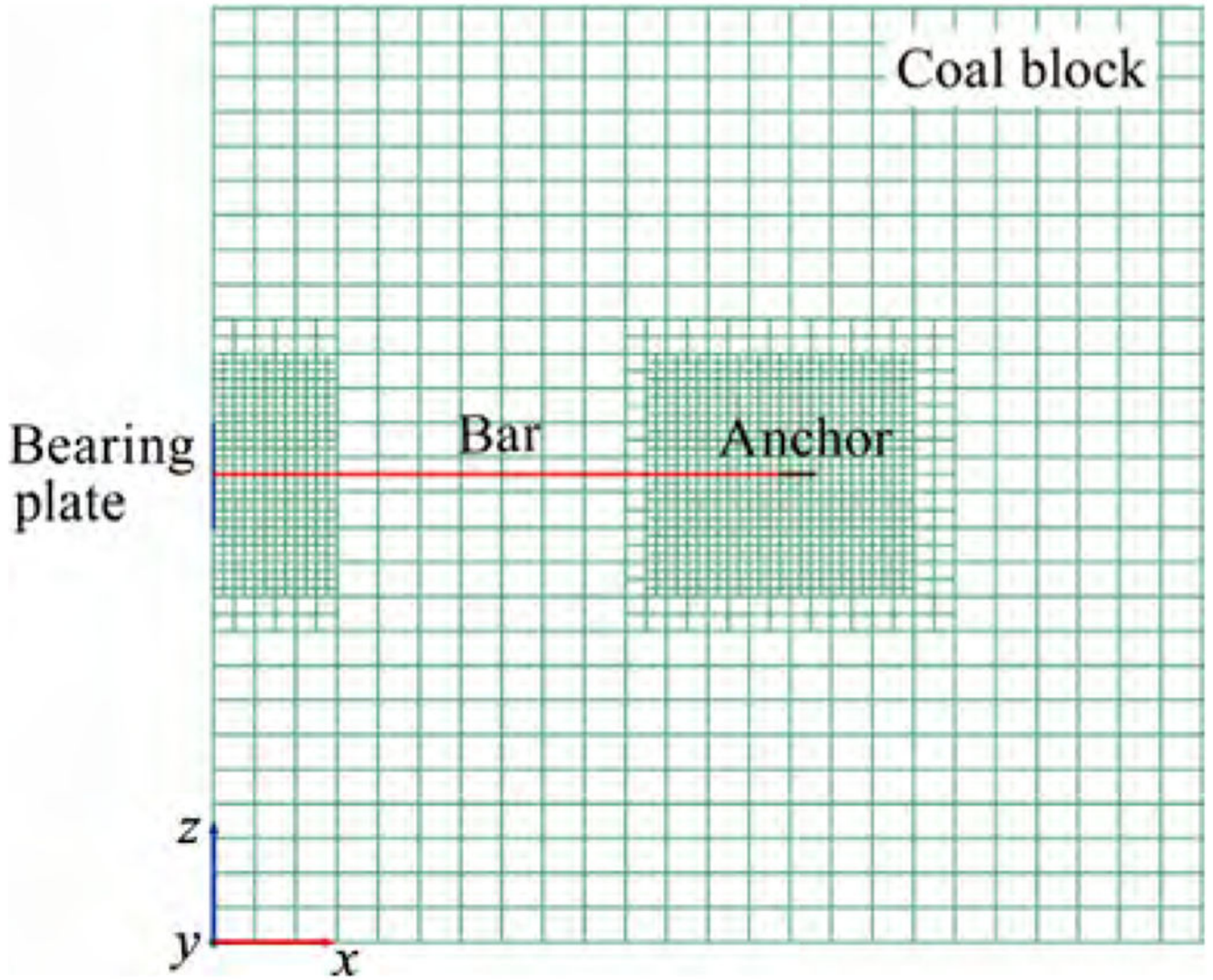


Fig. 9. Typical load-displacement curves at different installation torques.



**Fig. 10.** Reduced and calculated tri-linear load-displacement model of Test #1 at Mine B.



**Fig. 11.**  
The FLAC3D model for a 1.2 m long mechanical bolt installed in a 2 m coal block.

**Table 1**

Summary of critical points of tri-linear load-displacement models [18].

Mine	UCS (MPa)	Test #	Torque (kN-mm)	Point b		Point c		Point d' Load (kN)	Pre-tension load (kN)	Anchorage stiffness (kN/m)
				Disp. (mm)	Load (kN)	Disp. (mm)	Load (kN)			
NIOSH research mine	13.53	1	102	1.27	23.1	15.75	40.6	21.3	10.4	1213
		2	102	1.52	23.0	15.49	31.2	23.0	17.9	584
		3	102	1.52	25.6	16.00	36.8	26.0	18.2	769
		4	136	1.27	26.9	10.41	35.2	28.1	19.6	906
		5	136	0.76	30.5	4.83	37.2	29.3	20.5	1651
		6	136	1.27	30.5	11.18	45.4	29.5	20.6	1498
		7	163	0.51	34.7	3.81	42.6	33.6	23.5	2394
		8	163	0.51	30.4	3.56	36.1	30.2	21.2	1867
		9	163	1.52	29.3	3.56	32.3	27.4	19.2	1475
Mine A	5.79	1	102	0.25	22.2	2.54	25.8	22.2	15.6	1557
		2	102	0.25	23.6	22.86	40.0	21.4	14.9	728
Mine B	17.24	1	136	1.52	28.9	15.24	57.8	26.7	18.7	2108
		2	136	1.02	28.9	20.32	64.5	26.7	18.7	1843
		3	163	1.27	36.9	15.24	62.7	35.6	24.9	1847
Mine C	19.81	1	136	1.27	36.9	17.78	59.2	26.7	24.9	1347
		2	136	0.76	29.8	17.78	62.3	28.9	20.2	1908
		3	136	1.02	28.9	17.78	62.3	26.7	18.7	1990
Mine D	31.95	1	163	1.02	40.0	20.32	97.9	37.8	26.5	2996
		2	163	0.76	48.9	16.51	80.1	46.7	32.7	1977
		3	163	1.52	40.0	25.40	80.1	37.8	26.5	1677
		4	163	2.29	35.6	21.59	80.1	29.4	20.6	2304

**Table 2**

Physical and mechanical properties of the mechanical bolt used in the model.

Parameter	Value
Bolt length (m)	1.2
Anchor (grout) length (mm)	76
Free length (non-grouted) (m)	1.124
Bolt diameter (mm)	16
Hole diameter (mm)	35
Young's modulus of steel (GPa)	200
Yield load (kN)	102
Cohesion (grout) (kN/m)	823
Grout stiffness (Line <i>d-b</i> ) (MN/m <sup>2</sup> )	171
Grout stiffness (Line <i>b-c</i> ) (MN/m <sup>2</sup> )	30
Friction angle (grout) (°)	0
Cohesion (non-grouted) (MN)	0
Stiffness (non-grouted) (MN/m <sup>2</sup> )	0

**Table 3**

Mechanical properties of the coal-mass used in the model.

Parameter	Value
Young's modulus (GPa)	2.55
Poisson's ratio	0.25
Intact compressive strength (MPa)	22.0
Coal-mass scale	20
Fracture plastic shear strain	0.0375
Fracture plastic tensile strain	0.00375
Friction angle of fracture plane (°)	25
Cleat orientation with respect to x-direction (°)	90

Author Manuscript

Author Manuscript

Author Manuscript

Author Manuscript